

Date of publication xxxx 00, 0000, date of current version xxxx 00, 0000.

Digital Object Identifier 10.1109/ACCESS.2017.Doi Number

Efficiency Analysis of a Truncated Flip-FBMC in Burst Optical Transmission

MOHAMMED S. BAHAAELDEN¹, BEATRIZ ORTEGA¹, (Member, IEEE), RAFAEL PÉREZ-JIMÉNEZ², AND MARKKU RENFORS³, (Fellow, IEEE).

¹Telecommunications department, School of Engineering, Optical and quantum communications Team, politicianly university of Valencia, 46022 Valencia, Spain

²Institute for Technological Development and Innovation in Communications (IDeTIC), University of Las Palmas de Gran Canaria, 35001 Las Palmas, Spain

³Department of Electronics and Communications Engineering, Tampere University of Technology, 33720 Tampere, Finland

Corresponding author: Mohammed S. Bahaaelden (moba2@doctor.upv.es).

This work was supported by the Spanish Ministerio de Ciencia, Innovación y Universidades RTI2018-101658-B-I00 FOCAL project; the COST action NEWFOCUS (CA19111); and the Spanish Research Agency, project TEC2017-84065-C3-1-R.

ABSTRACT A novel Flip-filter bank multicarrier (Flip-FBMC) based transmultiplexer (TMUX) with offset quadrature amplitude modulation is proposed to enhance the Flip-OFDM performance. Moreover, the possibility to reduce the TMUX response (latency) and increase the gain in the spectral efficiency have been investigated for the first time through a tail shortening method. The proposed design is based on a biorthogonal form for visible light communication (VLC) to increase the flexibility degree of the design requirements. However, the spectral efficiency is detected to be suffering from the ramp-up and the ramp-down at the beginning and end, respectively, of the data burst. Hence, as penalty, Flip-FBMC imposes 9-extra symbols than Flip-OFDM packet and two-factor compared to DCO-FBMC burst. A hard truncation for the lowest energy tail contributes to minimize the latency and limits the system penalty to 2.5 symbols which is lower than DCO-FBMC by 2 symbols. The results show that the prototype filter of Heisenberg factor (≈ 1) is highly desired to reduce the energy loss of truncated tail and improves the symbol error rate (SER) performance. The Flip-FBMC over a direct line-of-sight VLC channel gain is analyzed and, the channel estimation of truncated burst, which based on the interference approximation method (IAM) of IAM-C type, exhibits a superior performance of 1.5 dB at 10^{-3} SER over IAM-R method and 1dB at 10^{-5} SNR over a cyclic prefix of 1 point Flip-OFDM. On the other hand, the analysis reveals that IAM-C are slightly impacted by the burst cut compared to the nontruncated model.

INDEX TERMS Filter bank multicarrier (FBMC), hard truncation methods, Heisenberg factor, interference approximation method, visible light communication (VLC), Flip-OFDM

I. INTRODUCTION

In the recent years, visible light communication (VLC) has attracted a lot of attentions due to immunity to electro-magnetic interference, free-health hazard and unlicensed spectrum. Besides, it is rapidly emerging as a compelling technology for supplementing conventional radiofrequency (RF) communication [1].

The most widespread modulation techniques in VLC, based on a unipolar-real time signal, are DC-offset orthogonal frequency division multiplexing (DCO-OFDM), asymmetric clipped optical OFDM (ACO-OFDM) and Flip-OFDM [2]-[3]. DCO-OFDM scheme requires a DC-bias voltage to transform a bipolar-real optical signal to unipolar form in order to be employed in intensity modulation and direct detection (IM/DD) communication systems

at the expense of high peak to average power ratio (PAPR) specially for large constellation signals, so the clipping noise must be low to achieve high optical power and SNRs [4]. Furthermore, the use of large values of V_{DC} leads to an inefficient optical power, whereas the use of low V_{DC} results in a significant out-of-band optical power and an enormous inter-carrier interference (ICI).

Flip-OFDM has a superior performance over the well-known DCO-OFDM at the expense of 50% bandwidth penalty [5]. Moreover, Flip-OFDM shows identical BER/SNR performance to ACO-OFDM technique, but with 50% less receiver hardware complexity [6]. As it is well known, OFDM subcarrier bands exhibit large sidelobes which, under interferences, may lose the orthogonality, and the power leakage of one of them can be high enough to disable several neighbor channels. Additionally, the

insertion of cyclic prefixes (CPs) in order to eliminate the inter symbol interference (ISI) in OFDM of rectangular pulses, which are very sensitive to synchronization errors, drives to both spectral and power efficiency reduction [7]-[8].

OFDM with offset quadrature amplitude modulation (OFDM/OQAM), also known as filter bank based multicarrier (FBMC), has been considered as an attractive alternative to the traditional OFDM because of its ability to reduce the out-of-band power leakage, boosting the gain in spectral efficiency, and overcoming the limitations arising from synchronization errors.

Furthermore, OFDM/OQAM has been adopted and modified as DC offset FBMC (DCO-FBMC) for VLC in [9], where the information rate has been increased by 9% because of elimination of 16-CP symbols overhead and guard bands. Although the influence of intrinsic imaginary interference (IMI), which is considered as the major obstacle in FBMC mechanism, the error performance is found to be identical to DCO-OFDM by using an isotropic orthogonal transformation algorithm (IOTA) filter with a channel estimation (CE) based on the Interference Approximation Method (IAM) of IAM-R type.

However, the CE based IAM-C type is assessed as the optimum choice for signal estimation (2dB better performance over OFDM in RF field [10]), inasmuch as its pseudo-pilots have larger magnitude than IAM-R, and lower PAPR compared to other CE based preambles (i.e., the extended IAM-C, IAM-R and other interference cancellation methods) [11]-[12]. From such a perspective, the preamble has been introduced in coherent optical communications [13]-[14].

DCO-FBMC has also exhibited a superior bit error rate performance over the traditional technique by using Mirabbasi-Martin filter and pilot-aided CE to combat IMI [15], while DCO-OFDM required CP of one sample to combat ISI over free space of 20 cm line of sight (LOS) distance using laser diode at 642 nm. However, FBMC/OQAM signals exhibit a penalty in terms of the number of symbols to transmit due to the transitions of the redundancy tails at both sides of data burst, which leads to a reduction in the spectral efficiency and therefore, a significant throughput reduction specially in short packets transmission. In RF domain, several methods were proposed to increase the spectral efficiency, such as a hard truncation method [16], despite it degrades the system performance using PHYDYAS filter (Martin filter with overlapping factor $K = 4$). For a given application, the performance of a prototype filter is evaluated through some of its figures of merit, such as the Heisenberg parameter (ζ), which is a measure of how well the localized pulse deals with such a harsh environment [17]-[18].

In this work, for the first time to the authors knowledge, we propose a novel Flip-FBMC scheme based transmultiplexer (TMUX) model in [19] as a good alternative for the traditional Flip-OFDM technique in [3]. The scheme is based on a biorthogonal form to increase the flexibility degree of the design requirements. Furthermore, a modified hard truncation method of the redundancy-tail will be investigated to be employed in VLC system for the first time in order to increase the information rate and reduce the reconstructed delay (TMUX response) at AFB output. Moreover, the truncation impact is evaluated according to the quality of the retrieved signal. The analysis comparison

between IOTA and Martin filters based on their Heisenberg factor leads to select the optimum one over the proposed-shortened tails and different modulation orders. In Flip-FBMC, the two variants of the IAM methods in [11] will be employed to mitigate the IMI influence, and enhance the accuracy of CE over the conventional Flip-OFDM technique. Besides, the performance of truncated system with IAM-R and IAM-C preambles are reported with respect to nontruncated version.

The rest of this paper is structured as follows. In section II, we introduce a biorthogonal Flip-FBMC modulation format for IM/DD LOS optical system. Section III presents the results of the performance and comparison to Flip-OFDM. Section IV exhibits a tail shortening method to further improve the spectral efficiency and TMUX-response. Section V presents the estimation of indoor LOS channel state information by using a one-tap zero forcing equalization (ZF) with IAM-R and IAM-C channel estimation methods, both based on truncated burst transmission. Finally, the concluding remarks are provided in section VI.

II. FLIP FBMC-TMUX SYSTEM DESCRIPTION

FBMC-TMUX is considered a biorthogonal system with a sufficient flexibility in the design requirements since either Inverse Fast Fourier Transform (IFFT) or Fast Fourier Transform (FFT) can be employed at the receiver (RX) side [20]-[21], where both designs still share the same performance results. The core of the FBMC system is the TMUX configuration with the fundamental processing blocks of OQAM pre-processing, and synthesis filter bank (SFB) that combines sub-band signals into one filtered signal. At RX side, the analysis filter bank (AFB) includes the matching receiver filters and OQAM post-processing allows to retrieve the complex input signal [22]-[26]. The schematic diagram of Flip-FBMC based on a biorthogonal form for a VLC system is depicted in Fig. 1, which shows the flexibility at the RX side, where either RX_1 or RX_2 is needed to retrieve the input signal. The bipolar-FBMC signal $X(k)$ at the transmitter (TX) side can be expressed as follows [21]:

$$X(k) = \sum_{n=0}^{N-1} \sum_{m=0}^{M-1} A_{m,n} P_{m,n}[k]$$

$$X(k) = \sum_{n=0}^{N-1} \sum_{m=0}^{M-1} A_{m,n} \varphi_{m,n} \underbrace{e^{-j \frac{2\pi m (M^*K+1)-1}{2} \rho_n}}_{\rho_n} * p \left[k - n \frac{M}{2} \right] e^{j 2\pi \frac{mk}{M}} \quad (1)$$

with

$$\varphi_{m,n} = e^{j \frac{\pi}{2} (m+n)} = j^{(m+n)} \quad (2)$$

where M denotes the total number of subchannels in the filter bank, which equal to $(2*(M/2-1)+2)$ subcarriers due to the Hermitian symmetry that given in table 1, N is number of total employed symbols. While $P_{m,n}[k]$ describes the pulse shape of the prototype filter, and $A_{m,n}$ are two staggered of pulse amplitude modulation (PAM) symbols. The phase shift term between adjacent PAMs is indicated by $\varphi_{m,n}$.

The OQAM staggering block is calculated according to [24], [26] as:

$$A_{m,2n} = \begin{cases} \text{Re}[C_{m,n}] & m \text{ even} \\ \text{Im}[C_{m,n}] & m \text{ odd}, \end{cases} \quad (3)$$

and

$$A_{m,2n+1} = \begin{cases} \text{Im}[C_{m,n}] & m \text{ even} \\ \text{Re}[C_{m,n}] & m \text{ odd}, \end{cases} \quad (4)$$

The complex to real conversion-block ($C2R_{m,n}$) converts the input symbol of a complex QAM ($C_{m,n}$) into real adjacent symbols with $T/2$ of relative time offset in order to carry the quadrature and in phase information of the input-complex QAM. Hence, the staggering process results in up-sampling by factor of 2.

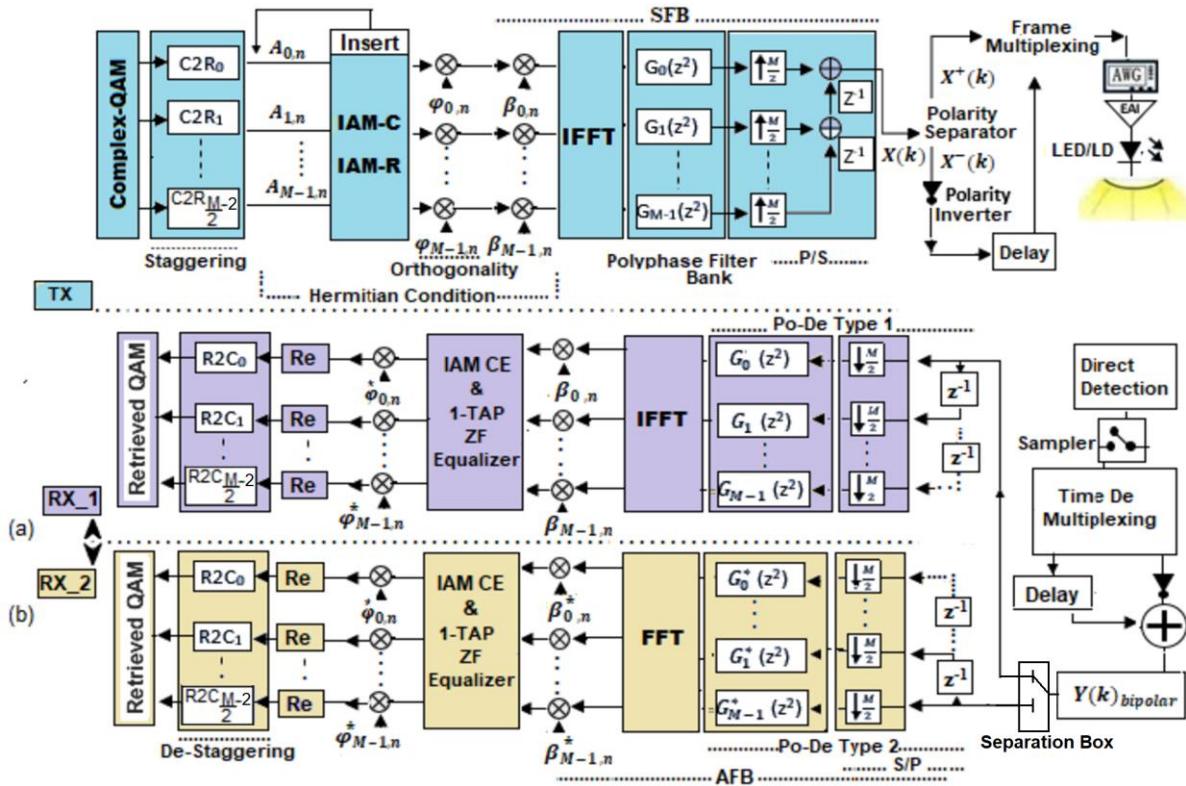


FIGURE 1. Polyphase implementation of a biorthogonal Flip-FBMC based TMUX configuration in VLC system to recover the input-QAM signal by using : either (a) IFFT based RX_1 or (b) FFT based RX_2.

The real-successive symbols $A_{m,n}$ are $\pi/2$ phase shifted using $\varphi_{m,n}$ to preserve the orthogonality. In order to obtain a real-bipolar signal in FBMC-TMUX transmitter side, the

orthogonal-complex symbols with corresponding phase-shift of β_m must satisfy Hermitian symmetry conditions, as presented in Table 1.

TABLE 1. Hermitian symmetry of input signal in Flip- FBMC based TMUX structure.

		Symbol Number			
		1	2	...	2N
Subcarrier Number	1	0	0	0	0
	2	$\text{Re}(A(2,1)) \beta_2$	$J * \text{Im}(A(2,2)) \beta_2$...	$\varphi_{2,2N} * \text{Im}(A(2,2N)) \beta_2$
	3	$J * \text{Im}(A(3,1)) \beta_3$	$-1 * \text{Re}(A(3,2)) \beta_3$
	4	$-1 * \text{Re}(A(4,1)) \beta_4$	$-J * \text{Im}(A(4,2)) \beta_4$
	5	$-J * \text{Im}(A(5,1)) \beta_5$	$\text{Re}(A(5,2)) \beta_5$

	M/2+1	0	0	0	0

	M-1	$(J * \text{Im}(A(3,1)) \beta_3)^*$	$(-1 * \text{Im}(A(3,2)) \beta_3)^*$
	M	$(\text{Re}(A(2,1)) \beta_2)^*$	$(J * \text{Im}(A(2,2)) \beta_2)^*$...	$(\varphi_{2,2N} * \text{Im}(A(2,2N)) \beta_2)^*$

Provided Hermitian symmetry is satisfied between incoming signal and its transpose-conjugate feeding the IFFT processing block. Hence, the bipolar-real signal is obtained to be processed convolutionally by a bank of M uniform-shifted replicas of a prototype filter, which are symmetrical-real valued and delayed by $((M*K+I)-1)/2$ samples to provide the required causality. The $(M*K+I)$ term indicates the filter length with K overlapping factor, which controls the number of symbols that overlap in time domain. The biorthogonal system refers to the possibility of retrieving the transmitted signal either by IFFT based AFB at the first receiver (RX_1) by using type-1 polyphase decomposition (Po-De) as shown in Fig. 1(a) or FFT based AFB by employing polyphase filters of type-2 at the second receiver (RX_2) shown in Fig. 1(b). The synthesis filters $g_m(k)$ represent the m^{th} shifted version of prototype filter $p[k]$ of L_p length at transmitter side, while $f_m(k)$ is the m^{th} analysis filter at the receiver. Through type-2 Po-De, the $f_m(k)$ represents a complex-conjugated and time-reversed model of synthesis filter [18], as follows :

$$g_m(k) = p[k] e^{j2\pi \frac{mk}{M} \frac{L_p}{(M*K+I)-1}}$$

$$f_m(k) = g^* [L_p - 1 - m] \quad (5)$$

It is noteworthy mentioning that IFFT based AFB is very straightforward to implement, as no extra flipping required as in type-2 Po-De, but in order to emphasize the link and provide better backward compatibility to OFDM, FBMC-TMUX is practically deployed with FFT based AFB [21]-[22].

The bipolar FBMC signal $X(k)$ is obtained by up-sampling ratio of $M/2$ to compensate the rate loss due to the $T/2$ of relative time offset for OQAM mapping, followed by combining sub-band signals into one real-filtered signal, and this process called parallel to serial conversion (p/s) [25]. The $X(k)$ signal mutates to unipolar format as $X^+(k)$ and $X^-(k)$ utilizing flip processing technique, which are juxtaposed in consecutive FBMC-subframes to be employed for IM of the LED, and can be calculated according to [3], [6]:

$$X^+(k)_{\text{Positive_part}} = \begin{cases} x(k) & \text{if } k \geq 0 \\ 0 & \text{otherwise} \end{cases}$$

$$X^-(k)_{\text{Flipped_part}} = \begin{cases} x(k) & \text{if } k < 0 \\ 0 & \text{otherwise} \end{cases} \quad (6)$$

The successive-received FBMC subframes $Y^+(k)$ and $Y^-(k)$ are subtracted to regenerate the bipolar form, as:

$$Y(k)_{\text{FBMC_bipolar}} = \underbrace{X^+(k) \otimes h^+(l) + Z^+(k)}_{Y^+(k)} - \underbrace{(X^-(k) \otimes -h^-(l) + Z^-(k))}_{Y^-(k)} \quad (7)$$

where \otimes represents convolution, $h(l)$ is an optical-channel impulse response with l taps, and Z represents noise samples of additive white Gaussian noise (AWGN). The n^{th} non-equalized received symbols of m^{th} subcarriers can be achieved by demodulating the received signal given in Eq.(7) as [9], [27]:

$$R_{m,n} = \sum_{k=-\infty}^{\infty} Y(k) P_{m,n}[k]^*$$

$$R_{m,n} = H_{m,n} A_{m,n} + j^* \underbrace{\sum_{m_0, n_0 \in \Omega} H_{m_0, n_0} A_{m_0, n_0} \langle P_{m,n}[k], P_{m_0, n_0}[k] \rangle}_{\text{Intrinsic interference}}$$

$$+ \sum_{k=-\infty}^{\infty} \underbrace{Z(k) P_{m,n}[k]^*}_{Z_{m,n}}$$

$$R_{m,n} = H_m A_{m,n} + H_m j A_{m,n}^{\text{intrinsic}} + Z_{m,n} \quad (8)$$

where H_m is the m^{th} channel frequency response at the frequency-time (FT) point (m,n) , $Z_{m,n}$ denotes the gaussian noise, and Ω indicates the set of FT point around (m,n) . Extra attention is required at TMUX-receiver side, the delay parameter $\Delta\delta$ arises to ensure the causality, while the reconstructed delay (TMUX-latency) ΔY has been introduced at the evaluated symbols, and can be written as:

$$\Delta Y = \frac{2}{\text{IFFT}_{\text{Size}}} (L_p - 1 + \Delta\delta) \quad (9)$$

These parameters depend on the used filter-length, where a longer prototype drives to higher latency at TMUX-output [17], [22]. Interferences can be generated as imaginary intrinsic interference (IMI) $j A_{m,n}^{\text{intrinsic}}$ through the m^{th} multipath channel, which is inherent in FBMC mechanism and not possible to be prevented. On the other hand, the real self-interference can be avoided by using well-designed prototype filter [27]-[28]. From (8), the intrinsic interference term is purely imaginary if channel response is 1, and the received signal can be derived as :

$$A_{m,n}^{\text{Received}} = \text{Re} \{ R_{m,n} \} \quad (10)$$

Then, the input complex QAM symbol can be retrieved using real to complex conversion-block ($R2C_{m,n}$), as expressed in [26].

$$C_{m,n}^{\text{Retrieved}} = \begin{cases} A_{m,2n}^{\text{Received}} + j A_{m,2n+1}^{\text{Received}} & m \text{ even} \\ A_{m,2n+1}^{\text{Received}} + A_{m,2n}^{\text{Received}} & m \text{ odd}, \end{cases} \quad (11)$$

III. PERFORMANCE ANALYSIS AT A DIRECT LOS VLC CHANNEL

The analysis performance of a novel Flip-FBMC based TMUX and the conventional one in [6] are assessed in terms of Symbol Error Rate (SER), spectrum efficiency and the computational complexity over various overlapping factors of different employed filters. Through simulation-experimental setup of LOS optical wireless link that tabulated in Table 2, the channel DC gain of LOS optical wireless link is considered, and can be calculated as follows [29]:

$$h_{\text{Los}} = \begin{cases} \frac{(Q+1)Ar}{2\pi d^2} \cos^{\theta}(\theta) T_s(\Psi) g(\Psi) \cos(\Psi) & 0 \leq \Psi \leq \Psi_c \\ 0, & \Psi > \Psi_c \end{cases} \quad (12)$$

where Ψ is the incident angle, θ is the irradiance angle, Ar is the

physical area of the photodiode (PD), where $g(\Psi)$ performs as the gain of the optical concentrator with half-angle FOV (field of view) of Ψ_C , $T_S(\Psi)$ is the gain of optical filter, and d represents the distance between the light-emitting diode (LED) and PD. The Q parameter describes the order of Lambertian emission with semi-angle at half power $\phi_{1/2}$, and can be calculated according to [29]-[31]:

$$Q = -\ln(2) / \ln(\cos \phi_{1/2}) \quad (13)$$

TABLE 2. Simulation-System Parameters.

Parameters	Value	
Utilised technique	Flip FBMC	Flip OFDM
Field of view (FOV)	60°	
Link distance	80 cm	
Gain of an optical filter	1.0	
Responsivity of PIN 1601FS-AC	0.2 A/W @ 450 nm	
Lens-refractive index	1.5	
Transmitted power	4.5 mW	
Area of PD	0.125 mm ²	
AWGN	Shot & Thermal noise	
IFFT size (M)	64 samples	
Constellation mapping	Low-High	
Prototype filter	Martin & IOTA	Rectangular
overlapping factor (K)	3,4 & 5	Non
Number of transmitted symbols	1-100	

The system SER is evaluated as a function of the electrical signal-to-noise ratio (SNR) as depicted in Fig. 2. In this work, the employed parameters to estimate the LOS channel gain are based on [30], where a blue μ LED of a peak wavelength equals to 450 nm is used and, the influence of shot and thermal noise are modelled as AWGN. The simulation results in section III and IV are obtained assuming the optical channel state information in (12) is known at the receiver.

The most common choices of filter lengths are $IFFT_{Size} * K$, $IFFT_{Size} * K - 1$, and $IFFT_{Size} * K + 1$, where $IFFT_{Size}$ performs one block of M subcarriers (one symbol = 1 block of M samples). In addition, the shorter/longer than those filter-values experience a degradation in system performance. The biorthogonal-proposed system is tested by using Martin filter in [15], which is obtained to have a length of $IFFT_{Size} * K + 1$, since it represents the optimum length-choice for reconstruction quality [31]. To evaluate the performance comparison, each overlapping factor ($K = 3$, $K = 4$ and $K = 5$) of the proposed system is tested on low to high constellation mapping.

It can be seen from Fig. 2 that the overlapping factor of 3 presents higher SER performance than the conventional technique with increasing the constellation order, while the overlapping factor of 4 is shown to be the optimum choice due to a slightly improved error performance compared to Flip-OFDM. Even though $K = 5$ introduces almost identical improvement to $K = 4$, the boosting in computational complexity, filter-latency, and gain reduction in spectral efficiency are the most significant drawbacks [22].

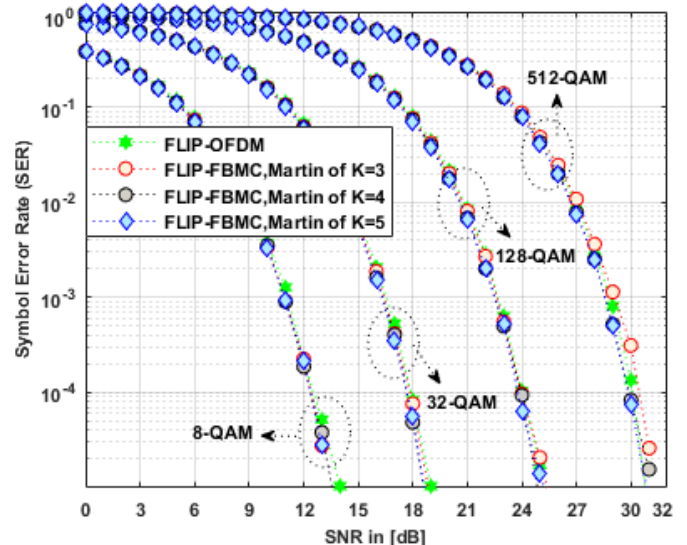


FIGURE 2. Performance comparison between Flip-FBMC of various overlapping factors and Flip-OFDM over different M-QAM modulation formats in VLC LOS-channel

The information-burst samples that will be conveyed over the modulation bandwidth of the LED, can be given by:

$$Flip - FBMC_{burst} = 2(IFFT_{Size} * (N + K + 0.5)) \quad (14)$$

The length of Flip-OFDM burst, with no-CPs and guard bands, is only $2 * (N IFFT_{Size})$ samples. Thus, Flip-OFDM exhibits higher spectral efficiency than the proposed scheme. However, a superior gain in spectral efficiency of optical FBMC compared to optical OFDM is experimentally reported, due to the utilised CPs and guard bands in optical OFDM structure to combat ISI [9].

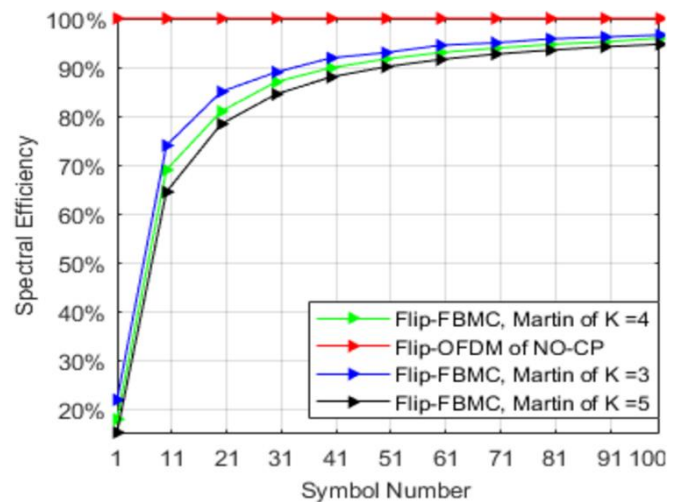


FIGURE 3. Spectral efficiency comparison at a flat-VLC channel

Fig. 3 shows the spectral efficiency of Flip-OFDM with no CP, and Flip-FBMC using Martin filter of different overlapping factors. It is observed that the spectral efficiency of the proposed approach boosts with reducing K and increasing the frame duration, where a limited packet exhibits a significant dropping in the information rate, inasmuch as the influence of redundancy

tails at both sides of packet data transmission. Thus, a tail shortening process performs an essential procedure to enhance the spectral efficiency, especially, for a short packet transmission [32] as detailed in section IV.

The power spectral density (PSD) of the proposed scheme is examined through evaluating the out-of-band emission (OOBE) with respect to the classical system. The major feature of FBMC is the low OOB radiation, allowing for more efficient spectrum sharing between users [33]. Fig. 4 illustrates the capability of the considered Flip-FBMC technique to reject the Flip-OFDM energy leakage of up to 50 dB, which also contributes to minimizing the synchronization errors.

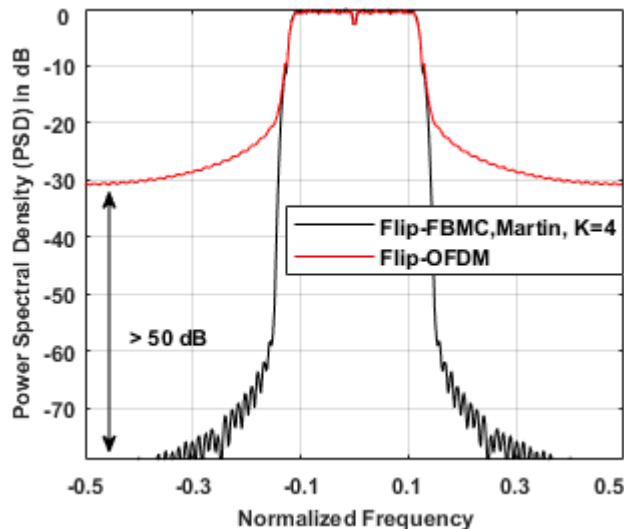


FIGURE 4. Power spectral density of Flip-FBMC vs Flip-OFDM.

The most significant drawback in FBMC-mechanism is the computational complexity [34]. However, regarding to [35], FBMC-TMUX based polyphase-systems represent less complexity than the one proposed in [15], due to the avoidance of unnecessary operations in frequency spreading technique. For the sake of comparison in terms of complexity in multiplication (M_{com}) and addition (A_{com}) terms require to transmit one block of symbol for both techniques using an FFT Split-Radix algorithm in [22], [35], and can be calculated as:

$$M_{com \text{ Flip-FBMC}} = 2 * \underbrace{(2IFFT_{Size})}_{\text{OQAM}} + \underbrace{\left(\frac{\beta}{\beta} \right)}_{\text{IFFT}} + \underbrace{\left(IFFT_{Size} (\log_2 (IFFT_{Size}) - 3) + 4 \right)}_{\text{SFB}} + 2L_p \quad (15)$$

$$A_{com \text{ Flip-FBMC}} = 2 \left(3IFFT_{Size} (\log_2 IFFT_{Size} - 1) + 4 \right) + 2IFFT_{Size} + 4(L_p - IFFT_{Size}) \quad (16)$$

$$M_{com \text{ Flip-OFDM}} = \underbrace{IFFT_{Size} (\log_2 (IFFT_{Size} - 3) + 4)}_{\text{IFFT}} \quad (17)$$

$$A_{com \text{ Flip-OFDM}} = 3IFFT_{Size} (\log_2 IFFT_{Size}) - 3IFFT_{Size} + 4 \quad (18)$$

As presented in the equations above, Flip-OFDM has much less hardware complexity than the proposed one because of extra β

term and M branch for each AFB and SFB for a given filter length. It can also be noticed that the hardware complexity of Flip-FBMC is slightly reduced by using lower overlapping factors. Besides, the shortest filter length of $(IFFT_{Size} * K - 1)$ is preferable in terms of complexity since β influence can be neglected [22].

IV. TAIL SHORTENING THROUGH A HARD TRUNCATION TECHNIQUE

Further spectral analysis is required to optimize the bandwidth efficiency of the proposed system and, consequently, a short packet transmission is considered to only gain a better insight for the impact of redundancy tail at both sides of the bipolar packet and the proposed shortening method, as depicted in Figs. 5, 7 and 8. By employing Flip-FBMC scheme, the information-burst samples expressed in (14) are bandwidth limited because of the long filter impulse response that, consequently, imposes a ramp-up (initial transition) of 1.5 symbols, and a rump-down (final transition) of 2.5 symbols at the beginning and end, respectively, of the bipolar-FBMC burst in addition to a half symbol of data packet transmission, which is required in Flip-FBMC mechanism. These overhead blocks, which are doubled due to the flipping process, lead to penalty and, consequently, to boost the gain-reduction in the spectral efficiency. Thus, the mechanism of Flip-FBMC, with $IFFT_{Size} * K + 1$ of filter length and $K=4$, imposes a penalty of $2 * (K + 0.5)$ extra symbols to transmit than Flip-OFDM burst of no CP.

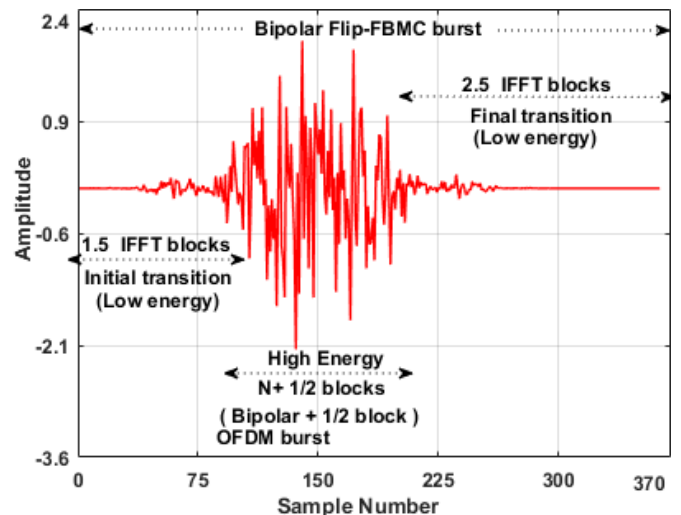


FIGURE 5. Bipolar-FBMC burst of a short packet (1-conveyed symbols).

The most significant parts of the transitions can be safely truncated since the average energy of these symbols are very small compared to the other higher energy of $(N + 1/2)$ bipolar FBMC-blocks [30]. Therefore, a hard truncation of the lowest energy tails (1.5 and 2.5 of IFFT-blocks) over a long burst data is considered to improve the gain in the spectral efficiency. It is noteworthy mentioning that with such shortening values, a minimum penalty of an extra half symbol is reached, which is doubled to one IFFT block more than the Flip-OFDM burst. However, the most redundancy-tails may be cut with minor influence [16]. Hence, the resulted truncation shows a noteworthy influence in run-down the quality of retrieved signal, as shown in Fig. 6.

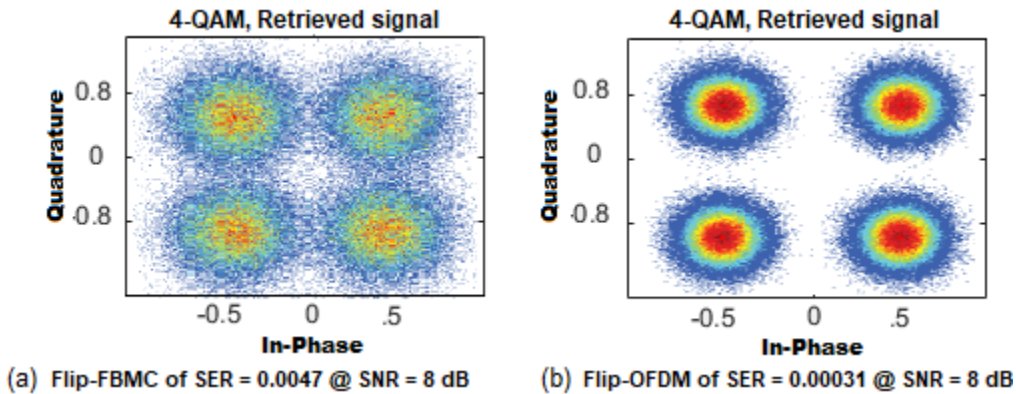


FIGURE 6. Constellations of 4-QAM retrieved signals over a long data-burst (100-transmitted symbols) to show (a) the degradation of the Flip-FBMC performance through a hard truncation of the lowest energy-parts (1.5 symbols at the packet beginning, and 2.5 symbols at end of data-burst) of tail, as compared to the classical Flip-OFDM for (b).

To maintain the proposed system identical to Flip-OFDM performance, and by using Monte Carlo algorithm, different truncations of the redundancy tail have been tested to obtain the optimum shortening values at both sides of the bipolar burst.

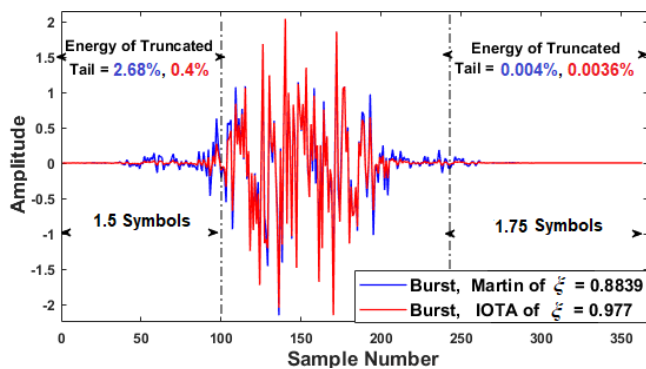


FIGURE 7. The optimal shortening values for the hard truncation method of 1.5, and 1.75 symbols at both sides of the short-bipolar burst.

As observed in Fig. 7, novel truncation values are obtained by leaving a part of redundancy tail at the beginning/end of the bipolar-FBMC packet, which significantly limit the interference level [30]. Thus, $1.5 * IFFT_{Size}$ (1.5 symbols) at the initial transition, and $1.75 * IFFT_{Size}$ (1.75 symbols) at the end of data burst are truncated away. Also, it depicts the distributed energy for the truncated tail at both sides of data packet, where the burst with MARTIN filter reduces the energy of data block further than what in IOTA. Notice that the assumed-truncated values are only valid with even overlapping factor ($K=4$) and ($IFFT_{Size} * K + 1$) of filter length. Therefore, the resulting length of FLIP-FBMC burst in samples can be determined as follows:

$$Truncated\ burst_{(even\ K)} = 2 * (IFFT_{Size} * (N + K - 2.75)) \quad (19)$$

The subframes ($X^+(k)$ and $X^-(k)$) of Flip-FBMC signal, as depicted in Fig. 8(a), impose a penalty of $2 * (4$ symbols) of extra IFFT blocks, and $2 * (0.5$ block) of an inherent tail. These 9 blocks of symbols (penalty) are minimized regarding to (19) to only 2.5 extra symbols than the conventional Flip-OFDM, as observed in Fig. 8(b).

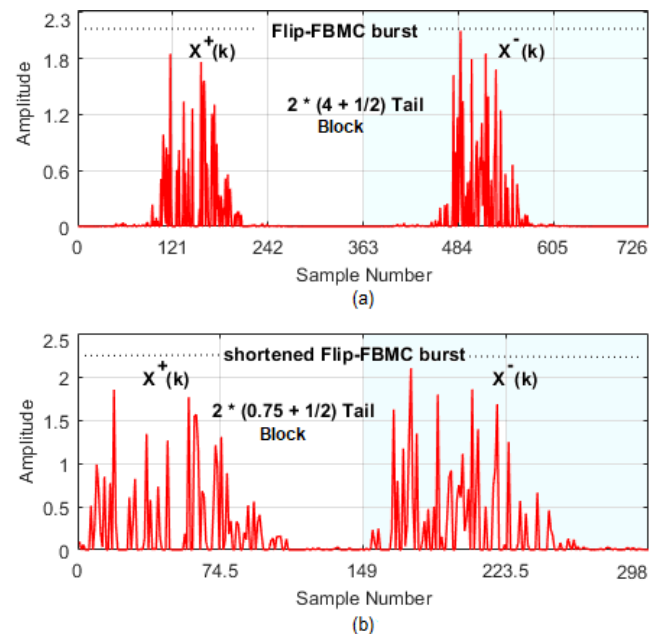


FIGURE 8. The consecutive subframes of Flip-FBMC burst for (a), and (b) the truncated version of Flip-FBMC packet.

The truncation burst using Martin-filter caused a remarkable degradation in system performance over a long data-burst (100-symbols) and high modulation orders (≥ 64 -QAM), while exhibits an identical SER performance to Flip-OFDM technique over lower mapping, as depicted in Fig. 9. To analyse the performance degradation of the proposed design, the characteristics of Martin-filter have been evaluated in terms of the figures of merit, which are presented in [17]. Martin filter showed a solid performance for various metrics for figures of merit, such as high quality of reconstructed signal, reliable signal to interference ratio and low OOB as presented in Fig. 10. To a certain extent, a low value of ζ factor is remarkable in Martin performance. Furthermore, it is also observed that this factor is improved by deploying a filter with a low time and frequency spreading [17]-[18]. From such a perspective, IOTA

filter in [17] with a near-optimum value of ξ is considered for sake of comparison. The exact ξ of the corresponding work using Martin and IOTA filters of length $IFFT_{Size} * K + 1$, can be measured as follows [17]-[18], [36]:

$$\xi = 1 / 4\pi \Delta W \Delta T \quad (20)$$

where

$$0 \leq \xi \leq 1 \quad (21)$$

The localization factor ξ is determined by the dispersion product of ΔW and ΔT , where the synthesis filters $g_m(k)$ have the same frequency dispersion (ΔW) and time dispersion (ΔT), which can be calculated as:

$$\Delta W = \sqrt{\int_{-\infty}^{\infty} f^2 |P(f)|^2 df} \quad (22)$$

and

$$\Delta T = \sqrt{\int_{-\infty}^{\infty} t^2 |p(t)|^2 dt} \quad (23)$$

where $p(t)$ term is the prototype pulse function, and $p(f)$ is its Fourier transform. Notice that employing a filter with ξ close to 1, results in optimum time-frequency pulse localization [18], [36]. As illustrated in Fig. 7, IOTA filter of 0.977 localization factor (close to 1) results in concentrating the signal energy according to envelope function around its centre, which leads to lower energy loss than what in Martin-filter of $\xi = 0.8839$ due to the hard truncation of redundancy tails. Consequently, the truncated packet using IOTA filter exhibits an identical SER performance to Flip-OFDM technique, and a superior performance over the shortening burst using Martin filter at high constellation mapping in a flat VLC-channel, as observed in Fig. 9.

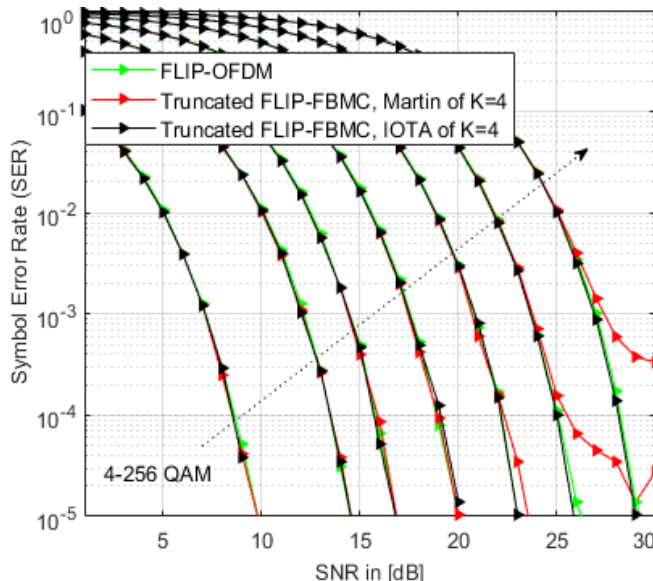


FIGURE 9. Symbol error rate vs SNR over a long data-burst for Flip-OFDM and Flip-FBMC employing IOTA and Martin filters of the proposed-truncated values of 1.5, and 1.75 symbols at both sides of the bipolar burst in a flat VLC-channel.

Moreover, it contributes to reduce the TMUX-latency that presented in (9), as:

$$\Delta T_{new} = \frac{2}{IFFT_{Size}} (L_p - 1 - 1.5 IFFT_{Size} + \Delta \delta) \quad (24)$$

where the $1.5 * IFFT_{Size}$ term is derived and added to satisfy the shortening in the packet data transmission. Thus, the reconstructed delay is reduced from $2K$ to $2K-3$ value at AFB output. The truncation effect on information rate can be observed in Fig. 10, where the throughputs of Flip-FBMC is highly dependent on the packet size (data blocks), and the gain in spectral efficiency is significantly improved at low numbers of IFFT blocks.

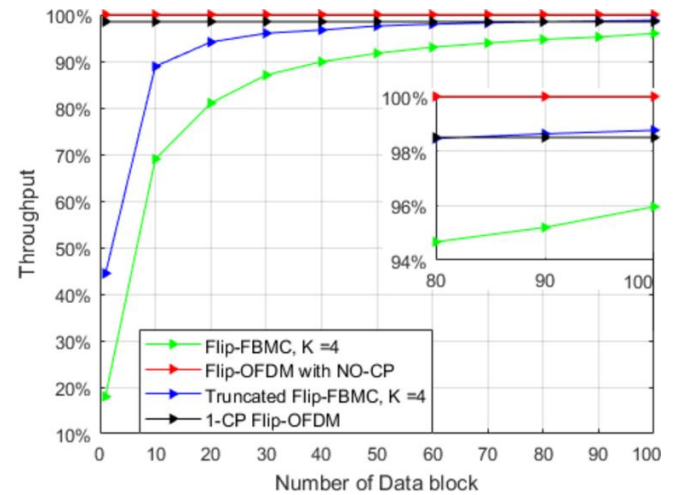


FIGURE 10. The hard truncation impact on the spectral efficiency.

V. ANALYSIS PERFORMANCE OF CHANNEL ESTIMATION

As described above, the optical FBMC has drawn a wide attraction because of the low out-of-band radiation arisen from well time-frequency localization of filter banks, and the high information rate that acquired by eliminating CPs and guard bands [37]. The performance of nontruncated/truncated Flip FBMC are evaluated with respect to the traditional one at the LOS channel gain that obtained in section III. In Flip-OFDM, a CP of 1 point length is added to combat ISI, and a one tap zero forcing (ZF) equalization based one training block of complex signal duration is used for CE, as detailed in Table 3.

TABLE 3. The system parameters for channel estimation parameters.

Parameters	Value	
	Flip FBMC	Flip OFDM
Utilised technique	Flip FBMC	Flip OFDM
IFFT size	64 samples	
Pilots duration in symbols	1.5	1
Constellation mapping	4-QAM	
Prototype filter	IOTA	Rectangular
Channel tap gain	1-Direct LOS	
CP size	0	1
Overlapping factor (k)	4	Non
Equalization size	1-Tap based CE of IAM-R/C	1-Tap
Number of Transmitted symbol	80 symbols	

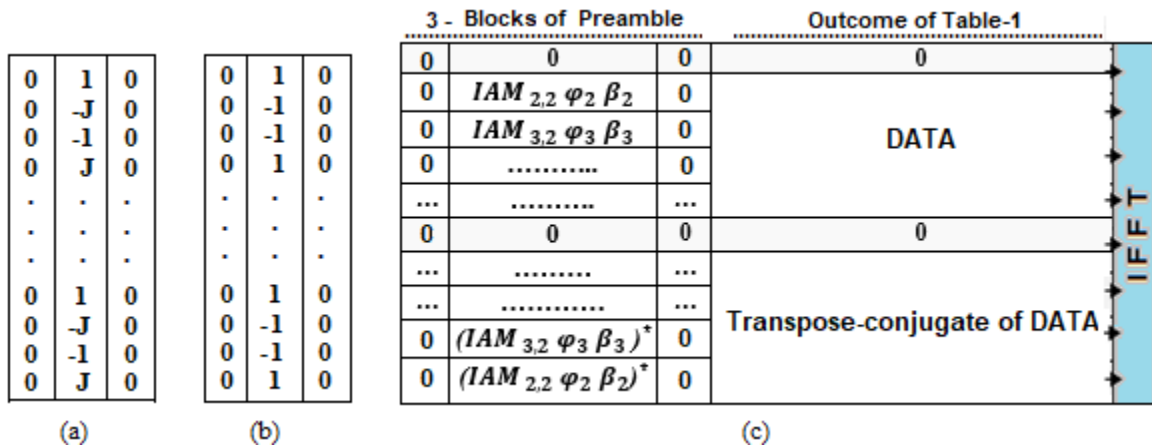


FIGURE 11. Preamble structures for (a) IAM-C, (b) IAM-R methods, and (c) Frame configuration for FBMC-TMUX VLC system

It can be seen from Fig. 11 that the CE of Flip-FBMC deployed the two variants of IAM (IAM-R and IAM-C) and inserted in the preamble in order to suppress the IMI effect. The length of three known sequential pilots equal to 1.5 training blocks (0.5 block more overhead than Flip-OFDM) that designed by inserting 2-blocks of zeros in the neighbourhood position of the maximize pilot power.

The 1st zero-block $P_{m0,n0-1}$ is employed to prevent interference from the previous frame and the two successive subframes at flipping stage. The nonzero part of transmitted pilots $P_{m0,n0}$ is set to the maximum value as presented in Fig. 11, while the 3rd block $P_{m0,n0+1}$ avoids interference from the payload data. The received preamble-pilots ($PLT_{m0,n0}$) can be performed as [11], [27]:

$$PLT_{m0,n0}^{received} = H_m \left(P_{m0,n0} + jP_{m0,n0}^{imaginary\ interference} \right) + Z_{m0,n0} \quad (25)$$

We have considered $N=80$, assuming a subframe of a VLC system. This assumption drives to an overhead of 1.55% residual tail and almost identical throughput to CP of one sample for Flip-OFDM, whereas creates around 5.7% blocks overhead for the nontruncated packet, as observed in Fig. 10. Further attention is required to obtain high data bit rate in real time transmission, as 3 dB modulation bandwidth of the commercially available LEDs is only several MHz [38]. The limited modulation bandwidth can be extended by using pre/post equalizations techniques [39].

The CE based IAM for Flip-FBMC VLC system can be computed as:

$$H_{m,n}^{\wedge} = \frac{PLT_{m0,n0}}{P_{m0,n0} + jP_{m0,n0}^{imaginary\ interference}} \quad (26)$$

The $jP_{m0,n0}$ term represents the interference weight which can be calculated in advance and restocked at the receiver with the aid of interference coefficients-FBMC law in [11]. Also, by using Monte Carlo algorithm and with respect to the traditional Flip-OFDM, the error performance of each nontruncated/truncated Flip-FBMC technique has been evaluated by using CE that based on IAM-R and IAM-C. A single tap ZF equalization is employed to nullify the LOS-

channel effects at the output of AFB, which can be calculated according to [9], [31].

$$A_{m,n}^{estimated} = \text{Re} \left\{ \left\langle \underbrace{Y(k), f_{m,n}(k)}_{AFB_output} \right\rangle \downarrow_M \underbrace{H_{m,n}^{\wedge}^{-1}}_{\frac{1}{2}} \right\} e^{-j\frac{\pi}{2}(m+n)} \underbrace{\phi_{m,n}^*}_{\phi_{m,n}^*} \quad (27)$$

It is noteworthy mentioning that

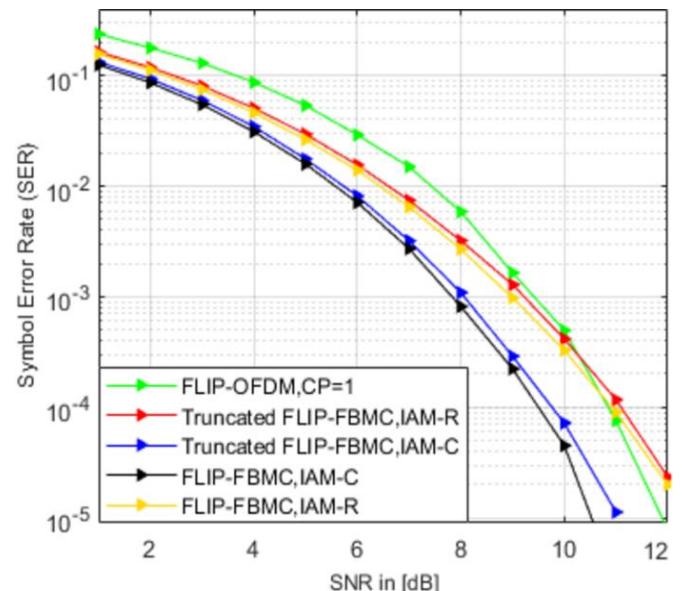


FIGURE 12. SER comparison between the truncated Flip-FBMC scheme and Flip-FBMC using CE based IAM-R/IAM-C compared with Flip-OFDM of 1-CP in LOS VLC-channel.

Fig. 12 shows the nonshortened/truncated-proposed design with IOTA filters of $K=4$, which are employed to be compared with the Flip-OFDM signals using 4-QAM modulation. The truncated Flip-FBMC based IAM-C exhibits a superior error performance of 1.5 dB at $SER=10^{-3}$, which decreases with increasing SNR values to reach 1dB at 10^{-3} SER compared to the traditional technique. However, the difference of the IAM-R performance compared to IAM-C is due to the required pseudo-

pilots in IAM-C method, which have larger magnitude than IAM-R and, hence, mitigate the impact of the additive gaussian noise and IMI effectively. Thus, the CE accuracy is further improved. On the other hand, the analysis exposes that the preamble-pilots based IAM-C are slightly impacted by the hard truncation of the transmitted burst with compared to the nontruncated version [15], while the shortening version using CE based IAM-R exhibits almost-identical SER performance to nontruncated one using IAM-R, inasmuch as the lower magnitude of pseudo-pilots related to the magnitude of IAM-C reference symbols. It is noteworthy mentioning that the function of Heisenberg factor in the shortening tails application has not been demonstrated before nor in RF field.

In future work, we will study the nonLOS propagation of different multipath scenarios in order to analyze the expected degradation of a single-tap equalizer and, the efficient multitap equalization will be investigated to improve the system robustness over larger delay spread. Additionally, a complex-valued symbol based FBMC/OQAM (C-FBMC/OQAM) model in [40] is tabulated to be proposed in IM/DD communication systems since C-FBMC/OQAM represents a key solution to imaginary interference cancellation, which demonstrated better performance over the conventional FBMC/OQAM system through frequency selective fading channels in RF field.

To support fifth generation (5G) applications requirement based on optical-FBMC, the proposed system can be efficiently deployed at indoor VLC, free space link-based LD and IM/DD passive optical network (PON) systems to enhance system performance [27], [41]. It is noteworthy mentioning that such a low latency is a crucial feature in the Tactile Internet (the next evolution of the Internet of Things) [42].

Although the flip-FBMC has lower PAPR than DCO-FBMC in [9] due to the required DC-bias voltage to obtain the unipolar form, it is noteworthy mentioning that the proposed scheme has higher PAPR than Flip-OFDM due to the deterministic sequences of IAM preamble [43]. However, this design model can be updated to efficiently reduce the PAPR, as presented in [44].

VI. CONCLUSION

In this work, for the first time to the authors knowledge, we introduce a Flip-FBMC scheme as a good alternative technique to enhance the performance of the traditional Flip-OFDM for the VLC systems. The proposed scheme is based on a biorthogonal form to provide the sufficient flexibility for a system design requirement. Moreover, the spectral efficiency has been increased by employing a hard truncation method for the redundancy tail with 1.5 symbols of the initial transition and 1.75 symbols of the final transition at both sides of data burst by using the optimum overlapping factor of 4 and $IFFT_{Size} * K + 1$ of filter length. Hence, the penalty of the proposed design has been reduced from $2*(K+5)$ to $2*(K-2.75)$ symbols, and the resulted penalty was lower than the DCO-FBMC penalty by 2 IFFT blocks. The impact of tail shortening has been evaluated over a long data burst by using IOTA and Martin filters, and as expected from low time and frequency spreading of IOTA filter

compared to Martin filter, the results showed concentration of the signal energy in an envelope function around its centre, which led to lower energy loss due to redundancy of truncated tail. Thus, employing a filter of Heisenberg factor close to one is considered one of the essential requirements in tail-shortening application. Hence, an identical SER performance has been obtained for Flip-FBMC by using IOTA filter to the traditional Flip-OFDM, while a significant degradation is reported at high modulation mapping with Martin filter when the optical channel state information is known at the receiver. Moreover, the truncated scheme contributed to reduce the TMUX latency from $2K$ to $2K-3$ at AFB output. The simulation results over a LOS channel gain showed that the truncated Flip-FBMC based IAM-C CE displayed a superior performance of around 1.5 dB at 10^{-3} SER which decreased with increasing SNR values to reach 1dB at 10^{-5} SER over the traditional Flip-OFDM of 1 CP, while the degradation in the accuracy of retrieved signal using IAM-R preamble has been addressed, since the magnitudes of the pseudo-pilots are lower than in IAM-R. On the other hand, the analysis revealed that the preamble-pilots based IAM-C are slightly impacted by the hard truncation with compared to the nontruncated model, while the shortening version using CE based IAM-R exhibited almost-identical SER performance to nontruncated one using IAM-R, due to the lower magnitude of IAM-R pseudo-pilots related to the magnitude of IAM-C reference symbols.

REFERENCES

- [1] D. C. O'Brien, L. Zeng, H. Le-Minh, G. Faulkner, J. W. Walewski and S. Randel, "Visible light communications: Challenges and possibilities," 2008 IEEE 19th International Symposium on Personal, Indoor and Mobile Radio Communications, Cannes, pp. 1-5, 2008.
- [2] S. D. Dissanayake and J. Armstrong, "Comparison of ACO-OFDM, DCO-OFDM and ADO-OFDM in IM/DD Systems," in *Journal of Lightwave Technology*, vol. 31, no. 7, pp. 1063-1072, April 1, 2013.
- [3] N. Fernando, Y. Hong and E. Viterbo, "Flip-OFDM for Unipolar Communication Systems," in *IEEE Transactions on Communications*, vol. 60, no. 12, pp. 3726-3733, December 2012.
- [4] J. Armstrong and B. J. C. Schmidt, "Comparison of Asymmetrically Clipped Optical OFDM and DC-Biased Optical OFDM in AWGN," in *IEEE Communications Letters*, vol. 12, no. 5, pp. 343-345, May 2008.
- [5] R. Islam, P. Choudhury and M. A. Islam, "Analysis of DCO-OFDM and flip-OFDM for IM/DD optical-wireless system," 8th International Conference on Electrical and Computer Engineering, Dhaka, pp. 32-35, 2014
- [6] N. Fernando, Y. Hong and E. Viterbo, "Flip-OFDM for optical wireless communications," 2011 IEEE Information Theory Workshop, Paraty, pp. 5-9, 2011
- [7] Q. He and A. Schmeink, "Comparison and evaluation between FBMC and OFDM systems," WSA 2015; 19th International ITG Workshop on Smart Antennas, Ilmenau, Germany, pp. 1-7, 2015
- [8] M. Bellanger, "FBMC physical layer: A primer", pp. 1-31, Jan. 2010. [online]. Available: <http://www.ict>

- phydyas.org/team-space/internal-folder/FBMC-Primer_06-2010.pdf.
- [9] B. Lin, X. Tang, Z. Ghassemlooy, X. Fang, C. Lin, Y. Li, S. Zhang, "Experimental demonstration of OFDM/OQAM transmission for visible light communications", *IEEE transactions on photonic*, vol. 8, no. 5, Oct.2016.
- [10] C. Lele, P. Siohan and R. Legouable, "2 dB Better Than CP-OFDM with OFDM/OQAM for Preamble-Based Channel Estimation," *2008 IEEE International Conference on Communications*, pp. 1302-1306, 2008.
- [11] E. Kofidis, D. Katselis, A. Rontogiannis, S. Theodoridis, "Preamble-based Channel Estimation in OFDM/OQAM Systems: A Review," *Signal Processing*, vol. 93, pp. 2038-2054, July 2013.
- [12] M. A. AboulDahab, M. M. Fouad and R. A. Roshdy, "A proposed preamble based channel estimation method for FBMC in 5G wireless channels," *2018 35th National Radio Science Conference (NRSC)*, Cairo, Egypt, pp. 140-148, 2018.
- [13] k. A. Alaghbari, H.-S. Lim and T. Eltaif, "An improved least squares channel estimation algorithm for coherent optical FBMC/OQAM system," *Opt. Commun.*, vol. 439, pp. 141-147, 2019. [Online]. Available: <https://doi.org/10.1016/j.optcom.2019.01.012>.
- [14] X. Fang *et al.*, "Analysis of the Time-Frequency Localization Property of the Filter Banks for Optical OFDM/OQAM Systems," in *Journal of Lightwave Technology*, vol. 37, no. 21, pp. 5392-5405, 1 Nov.1, 2019.
- [15] R. Chen, K.-H. Park, C. Shen, T. K. Ng, B. S. Ooi, M.-S. Alouini, "Visible light communication using DC-biased optical filter bank multi-carrier modulation", *IEEE Global LIFI Congress*, 19 March 2018.
- [16] M. Bellanger, "Efficiency of filter bank multicarrier techniques in burst radio transmission", *Global Telecommunications Conference*, pp. 1-4, Dec. 2010.
- [17] R. T. Kobayashi and T. Abrão, "FBMC Prototype Filter Design via Convex Optimization," in *IEEE Transactions on Vehicular Technology*, vol. 68, no. 1, pp. 393-404, Jan. 2019.
- [18] C. Boyd, R. Pitaval, O. Tirkkonen and R. Wichman, "On the time-frequency localisation of 5G candidate waveforms," *2015 IEEE 16th International Workshop on Signal Processing Advances in Wireless Communications (SPAWC)*, Stockholm, Sweden, pp. 101-105, 2015.
- [19] L. G. Baltar, I. Slim and J. A. Nossek, "Efficient filter bank multicarrier realizations for 5G," *2015 IEEE International Symposium on Circuits and Systems (ISCAS)*, Lisbon, pp. 2608-2611, 2015
- [20] P.P. Vaidyanathan: *Multirate Systems and Filter Banks*. Prentice-Hall, Englewood Cliffs, NJ, USA; 1993.
- [21] P. Siohan, C. Siclet and N. Lacaille, "Analysis and design of OFDM/OQAM systems based on filterbank theory," in *IEEE Transactions on Signal Processing*, vol. 50, no. 5, pp. 1170-1183, May 2002.
- [22] INFSO-ICT-211887 Project PHYDYAS, *Deliverable 5.1: Prototype filter and structure optimization*, Jan. 2009. [Online]. Available: <http://www.ict-phydyas.org/delivrables/PHYDYAS-D5-1.pdf/view>
- [23] T. Stitz, T. Ihalainen, A. Viholainen *et al.* "Pilot-Based Synchronization and Equalization in Filter Bank Multicarrier Communications," *EURASIP J. Adv. Signal Process.* 2010.
- [24] M. Aldababseh and A. Jamoos, "Estimation of FBMC/OQAM fading channels using dual Kalman filters," *the Scientific World Journal*, 2014, 586403. [Online]. Available: <https://doi.org/10.1155/2014/586403>
- [25] N. Van der Neut, B.T. Maharaj, F. de Lange *et al.*, "PAPR reduction in FBMC using an ACE-based linear programming optimization," *EURASIP J. Adv. Signal Process.* 2014. [Online]. Available: <https://doi.org/10.1186/1687-6180-2014-172>
- [26] A. Viholainen, T. Ihalainen, T. H. Stitz, M. Renfors and M. Bellanger, "Prototype filter design for filter bank based multicarrier transmission," *2009 17th European Signal Processing Conference*, Glasgow, pp. 1359-1363, 2009.
- [27] J. Shi, J. He, R. Zhang and Rui Deng, "Experimental demonstration of blind equalization for OFDM/ OQAM-VLC system," *Optical engineering*, vol. 58, Jun. 2019.
- [28] C. Chen and F. Maehara, "An enhanced MMSE subchannel decision feedback equalizer with ICI suppression for FBMC/OQAM systems," *2017 International Conference on Computing, Networking and Communications (ICNC)*, Santa Clara, CA, , pp. 1041-1045, 2017.
- [29] T. Komine and M. Nakagawa, "Fundamental analysis for visible-light communication system using LED lights," in *IEEE Transactions on Consumer Electronics*, vol. 50, no. 1, pp. 100-107, Feb. 2004.
- [30] M. Ijaz *et al.*, "Optical spatial modulation OFDM using micro LEDs," *2014 48th Asilomar Conference on Signals, Systems and Computers*, Pacific Grove, CA, pp. 1734-1738 2014.
- [31] D. William, M. Guerra and T. Abrão, "Efficient multitap equalization for FBMC-OQAM systems," *Trans Emerg Telecommun Technol*, vol. 30, vol. 12, 2019. [Online]. Available: <https://onlinelibrary.wiley.com/doi/10.1002/ett.3775>.
- [32] A. Zafar, M. A. Imran, P. Xiao, A. Cao and Y. Gao, "Performance evaluation and comparison of different multicarrier modulation schemes," *2015 IEEE 20th International Workshop on Computer Aided Modelling and Design of Communication Links and Networks (CAMAD)*, Guildford, pp. 49-53, 2015.
- [33] Z. He, L. Zhou, Y. Chen and X. Ling, "Filter optimization of out-of-band emission and BER analysis for FBMC-OQAM system in 5G," *2017 IEEE 9th International Conference on Communication Software and Networks (ICCSN)*, Guangzhou, pp. 56-60, China, 2017.
- [34] S. Taheri, M. Ghoraiishi, P. Xiao and L. Zhang, "Efficient Implementation of Filter Bank Multicarrier Systems Using Circular Fast Convolution," in *IEEE Access*, vol. 5, pp. 2855-2869, 2017.
- [35] A. Husam and Z. Kollár, "Complexity Comparison of Filter Bank Multicarrier Transmitter Schemes," *2018 11th International Symposium on Communication Systems, Networks & Digital Signal Processing (CSNDSP)*, Budapest, pp. 1-4, 2018.

- [36] R. Haas and J.-C. Belfiore, "Multiple carrier transmission with time-frequency well-localized impulses," *IEEE Second Symposium on Communications and Vehicular Technology in the Benelux*, Louvain la Neuve, Belgium, pp. 187-193, 1994.
- [37] Y. Fu, X. Fang, X. Sui, L. Zhang, D. Ding and X. Gao, "Analysis of the Pseudo Pilot in Optical OFDM/OQAM System," *2020 12th International Conference on Communication Software and Networks (ICCSN)*, Chongqing, China, , pp. 161-165. 2020.
- [38] D. H. Kwon, S. H. Yang and S. K. Han, "Modulation bandwidth enhancement of white-LED-based visible light communications using electrical equalizations", *Proc. SPIE 9387, Broadband Access Communication Technologies IX*, 7 February 2015.[Online]. Available: <https://doi.org/10.1117/12.2078680>
- [39] N. Fujimoto and H. Mochizuki, "477 Mbit/s visible light transmission based on OOK-NRZ modulation using a single commercially available visible LED and a practical LED driver with a pre-emphasis circuit," *Optical Fiber Communication Conference and Exposition and the National Fiber Optic Engineers Conference (OFC/NFOEC)*, Anaheim, CA, 2013.
- [40] D. Kong, X. Zheng, Y. Zhang and T. Jiang, "Frame Repetition: A Solution to Imaginary Interference Cancellation in FBMC/OQAM Systems," in *IEEE Transactions on Signal Processing*, vol. 68, pp. 1259-1273, 2020.
- [41] M. F. Sanya, L. Djogbe, A. Vianou and C. Aupetit-Berthelemot, "DC-biased optical OFDM for IM/DD passive optical network systems," in *IEEE/OSA Journal of Optical Communications and Networking*, vol. 7, no. 4, pp. 205-214, April 2015.
- [42] S. K. Sharma, I. Woungang, A. Anpalagan and S. Chatzinotas, "Toward Tactile Internet in Beyond 5G Era: Recent Advances, Current Issues, and Future Directions," in *IEEE Access*, vol. 8, pp. 56948-56991, 2020.
- [43] D. Kong, J. Li, K. Luo and T. Jiang, "Reducing Pilot Overhead: Channel Estimation With Symbol Repetition in MIMO-FBMC Systems," in *IEEE Transactions on Communications*, vol. 68, no. 12, pp. 7634-7646, Dec. 2020.
- [44] D. Kong, X. Zheng, Y. Yang, Y. Zhang and T. Jiang, "A Novel DFT-Based Scheme for PAPR Reduction in FBMC/OQAM Systems," in *IEEE Wireless Communications Letters*, vol. 10, no. 1, pp. 161-165, Jan. 2021.